Accepted Manuscript

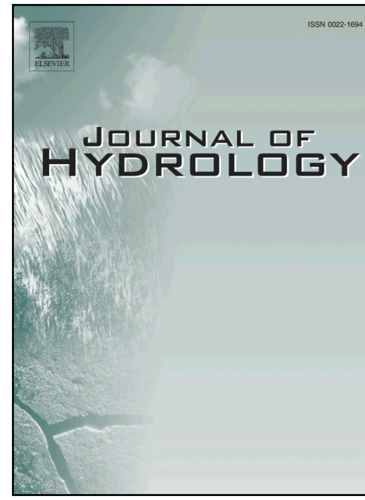

Research papers

Rainfall partitioning after thinning in two low-biomass semiarid forests: impact of meteorological variables and forest structure on the effectiveness of water-oriented treatments

Antonio D. del Campo, María González-Sanchis, Antonio Lidón, Carlos J. Ceacero, Alberto García-Prats

PII: S0022-1694(18)30609-7
DOI: https://doi.org/10.1016/j.jhydrol.2018.08.013
Reference: HYDROL 23027

To appear in: *Journal of Hydrology*

Received Date: 1 February 2018
Revised Date: 27 July 2018
Accepted Date: 6 August 2018

Rainfall partitioning after thinning in two low-biomass semiarid forests: impact of meteorological variables and forest structure on the effectiveness of water-oriented treatments

Antonio D. del Campo[a*], María González-Sanchis[a], Antonio Lidón[a], Carlos J. Ceacero[b], Alberto García-Prats[a]

a. Research Group in Forest Science and Technology (Re-ForeST), Research Institute of Water and Environmental Engineering (IIAMA), Universitat Politècnica de València, Camí de Vera s/n, E-46022 Valencia (Spain)

b. Departamento de Fisiología, Anatomía y Biología Celular, Universidad Pablo de Olavide, E-41013, Sevilla (Spain)

[*] Corresponding Author: ancamga@upv.es

Abstract

Water-oriented forest management is an urgent need in semiarid catchments. In the case of low-biomass forests and shrublands, the magnitude, efficiency and temporal duration of thinning effects on rainfall partitioning needs further attention. This work studies the effects of juvenile thinning and shrub clearing on stemflow (Stf), throughfall (Thr) and interception (It) in two low-biomass forests (CAL: post-fire Aleppo pine saplings with 74% of basal area, BA, removed; and HU: evergreen oak coppice with 41% of BA removed), as well as the relative contribution of the event meteorology. The effects are compared with a control plot during the first 3-4 years. Stf rate (%) decreased with density and, on a tree scale, it was enhanced by the treatment only in the bigger oaks. Event Thr increased from 55 to 81% and from 68 to 86% of gross rainfall (Pg) for CAL and HU respectively after thinning, resulting in about 15% less intercepted Pg. High evaporative conditions and an open (ventilated) forest structure led to high It rates in the controls when comparing with other studies, thus making the treatments more efficient in net precipitation (Pn) gain (Pg intercepted decreased 17% or 2.3% per unit of LAI or BA removed respectively). In general, depths (mm) were mostly explained (>75%) by the rainfall characteristics of the event (e.g. amount, duration, intensity), with a limited contribution from forest structure (e.g cover, LAI) and event meteorology (e.g. temperature, wind speed, vapor pressure deficit). On the contrary, when expressed as rates (% of Pg), forest structure and event-meteorology gained importance (explaining 25-65%), especially in the drier site (CAL). In this site, the low gain in Pn (~25 mm per year on average) was offset with no temporal dampening during the span of this study, as observed in the wetter site (HU), where plant growth tended to mitigate the effect of the treatment by the end of the study. The results presented here make a contribution to

a better understanding of the effects of water-oriented forest management in low-biomass semiarid forests.

Key words: adaptive silviculture, Aleppo pine *Pinus halepensis*, Holm oak *Quercus ilex,* interception, throughfall, stemflow, boosted regression trees.

1. Introduction

The impact of climatic and global changes on the ecosystem services of forests is a well-known documented fact that has gone much farther from research and science towards international policy actions, urging on the need of a sustainable forest management (UN, 2017). In spite that sustainable forest management is in the very roots of Silviculture (Carlowitz von, 1713, cit. in Schmithüsen, 2013), the targets and the strategies to maintain the principle of sustainability must be regionally tuned and adapted as novel changes in both the environment and the socio-economic conditions affect forests (Allen et al., 2015). In the context of global change-induced impacts, adaptive silviculture aims to adapt forests to new environmental conditions or especially to enhance resilience to changing disturbance regimes (Seidl et al., 2016). In semiarid forests, the focus of this adaptive silviculture must be necessarily eco-hydrologically founded and oriented, as water is the key element that links most of the global and climatic stressors affecting these ecosystems (del Campo et al., 2017), such as increased risk of drought stress and mortality, growth stagnation, blue/green water impairment, wild fire susceptibility, etc. (López et al., 2009; Klein et al., 2013; Grant et al., 2013; González-Sanchis et al., 2015; García-Prats et al., 2015; García de la Serrana et al., 2015; Fernandes et al., 2016). These water-driven stressors mutually interact and feedback with global change stressors such as the low value of forest products, rural abandonment, forest densification and encroachment, lack of forest management, etc. (Doblas-Miranda et al., 2017).

Low-biomass semiarid forests are especially prone to suffer from observed/projected trends in precipitation, temperature and evapotranspiration (Lindner et al., 2014) that may push many of them close to their distributional limit (Terradas and Savè, 1992; Peñuelas et al., 2017). However, they have been much less studied in the context of water-oriented forest management. Increasing net precipitation (decreasing interception loss) is usually the first target of water-oriented forest management in semiarid forests (Ungar et al., 2013; del Campo et al., 2014; Ilstedt et al., 2016). These studies claim a shift on the paradigm of full canopy cover to medium covers (40-50%) through selective thinning when implementing hydrology-oriented forest planning and management. In this sense, management tools conceived and designed for full cover (e.g. density diagrams, Valbuena et al., 2008) must be reconsidered within an approach of defective forest cover as an alternative. Forest and water relationships have been broadly studied and reviewed in semiarid forests (Llorens and Domingo, 2007; Levia and Germer, 2015) and studies dealing with rainfall partitioning have been published for decades (see reviews in Carlyle-Moses, 2004 and Swaffer et al., 2014), although those specifically addressing the effects of forest treatments such as selective thinning or shrub clearing are much scarcer, in particular in low-biomass forests (Table 1). Different effects can be expected according to the particular forest structure being treated and the meteorological characteristics of rainfall (Llorens et al., 1997; Crockford and Richardson, 2000; Mateos and Schnabel, 2001; Levia and Frost, 2003; Muzylo et al., 2012; Tanaka et al., 2015, 2017; Zabret et al., 2018). Accordingly, increased net precipitation in a cleared structure could be counterbalanced by higher wet evaporation under semiarid conditions (Dunkerley, 2000) so that the effectiveness of water-oriented forest management could be argued. Comparing to other forest types (e.g. temperate and sub-humid Mediterranean), low-biomass forests have distinctive values for most structural variables (e.g., aboveground biomass, canopy storage capacity, LAI, basal area, etc.), whereas for other variables (e.g., canopy cover, stem density, gap fraction, etc.), the differences may be more ambiguous. A question arising from this is whether the magnitude or rates of the structure-related hydrological processes, scale linearly to more complexly structured forests (Limousin et al., 2008).

In this context, gains in net precipitation after treatments must be necessarily explained in terms of the intensity of the treatments and this must be necessarily explained in terms of changes in structural variables. That is to say, it is necessary to address how much a particular hydrological process is significantly affected by silvicultural treatments, whether different structural variables (e.g., cover vs. LAI) are equally useful to explain the observed changes, and how much the role of climate (meteorological features of rainfall) affects these relationships (magnitude or rate of the structure-related hydrological processes). Studies addressing these questions may shed light on how forest-water interactions can be readily and efficiently manipulated in different semiarid contexts: forest-type and climate.

Unmanaged high-density stands of holm oak coppice and pine saplings regenerated after wildfires are common forest covers in the driest regions of Mediterranean Spain prone to climate-related disturbances (López et al., 2009; Doblas-Miranda et al., 2017), stressing the need to better define adaptive treatments in terms of intensity, frequency and efficiency. The major goal of this study is to quantify the effects of adaptive water-oriented forest management (thinning) on rainfall partitioning (stemflow, throughfall and interception) in two climatically and biologically contrasting low-biomass semiarid forests. The specific objectives of the research are: i) study rainfall partitioning in two low-biomass semiarid forest, i.e., are the magnitudes and rates of stemflow, throughfall and interception comparable to those reported for more mature and complex forest structures?; ii) assess the impact of forest treatments on rainfall partitioning, i.e., are the magnitudes and rates of stemflow, throughfall and interception after thinning comparable to those reported for more mature and complex forest structures?; iii) address the relative importance of forest structure and rainfall characteristics in rainfall partitioning and identify how much that importance changes with different site/climate conditions and biological structures (oak vs. pine); iv) evaluate the short to mid-term effect of the silvicultural interventions in rainfall partitioning. Table 1 presents a selected list of published literature on rainfall partitioning that share common topics to those covered in this study, and stresses the comprehensive combination addressed in the present work: i) the effect of forest management in low-biomass semiarid forests, ii) analysis of the relative importance of main drivers in Pg partitioning (Pg features, meteorology and forest structure), iii) two distant sites with marked differences in climate and vegetation that broaden the scope of the study, and iv) short to mid-term evaluation of the effects being studied.

2. Materials and methods

2.1. Study sites

The study was carried out in two contrasted low-biomass forest types located in the Valencia province (E Spain) distant about 100 km one to the other. Both sites differ not only in vegetation, but also in climate, rainfall characteristics, soils and other bio-geographical traits (Figure 1). The north-easternmost site, Calderona (CAL), is located in the Natural Park “Sierra Calderona”, which occupies part of the provinces of Valencia and Castellon following a general NW-SE orientation. The site has marked influence from the Mediterranean Sea, which is just 25 km away and presents Aleppo pine (*Pinus halepensis* Mill.) forests (saplings) regenerated after a wildfire occurred in 1992. The south-westernmost site is located in “La Hunde” (HU) public forest; it is occupied by marginal oak forest and has a pronounced continental climate (Table 2). The dominant species in this site is Holm oak (*Quercus ilex* ssp. *ballota* (Desf.) Samp.**)** and accompanying species are *Q. faginea*, *Pinus halepensis*, *Juniperus phoenicea* and *J. oxycedrus*. Although the climate is typically Mediterranean in both sites, there are important differences between them due to the continental vs. maritime influence (Table 2); Sierra Calderona is characterized by high temporal rainfall variability and intense droughts. In both sites, soils are relatively shallow (10-40cm), loamy textured, basic pH and have high calcium carbonate content (Table 2). Parent rock is karstified and there are no regular watercourses but numerous springs that may dry out in the summer months.

2.2. Treatments application, experimental layout and forest structure

This study was carried out at the plot scale as a basic land unit (pixel) useful to upscale to higher entity units (hillslope, forest stand, catchment). Both experimental sites share a common characteristic in the sense that tree density and competition is high (overstocked) and no forest management has been applied in the last decades due to their role of marginal and/or protective forests. Both sites exhibit low biomass forest types, with aboveground biomass estimated from allometric equations of 47.3 Mg/ha (22.2 Mg C/ha) in Calderona and 49.7 (23.1 Mg C/ha) in La Hunde, well below values in other Mediterranean and temperate forests (Pan et al., 2013). Juvenile thinning (CAL) and thinning with shrub clearing (HU) treatments were executed by a contractor of the Valencian Forest Service, following usual instructions and working methods (thinning from below). Thinning/clearing removed the trees with smaller diameters and doubled-trees and was performed to achieve a relatively homogeneous tree distribution (based on forest cover). Coarse woody debris were removed outside the plots whereas fine woody debris were piled and grinded into mulch onto the plots.

In CAL site, thinning works took place between January and October 2012 in an area of about 50 ha, with very high density of pine saplings (over 15000 stems ha^{-1}). In a representative area, one control (C) plot was left with no treatment and a contiguous treated (T) plot was established (October 2012). C and T plots were of 1500 m^2 respectively, both NW oriented (Table 2) and divided into 3 replicates or experimental blocks from upslope to downslope in order to assure representative results (Table 3). La Hunde site presents a coppice oak and shrubland forest as the result of traditional fuelwood harvesting that fell into disuse in the 1970's. This forest has high stem densities and, accordingly, high intraspecific competition that might be the responsible of top-tree dieback observed after severe dry years. In May 2012 an experimental thinning (tree with shrub clearing) was performed in a rectangular plot of about 1800 m^2 following the same criteria as in CAL (Table 3). Adjoining the thinned area, a control plot of similar size was established. Both plots were split into three blocks of similar size too.

Spatial forest structure was characterized by the proper metrics in both plots before and after the treatments. Total basal area removed in the treatments was 74% and 41% in CAL and HU, respectively, and density reduction was 94% and 73%, respectively. Over the ensuing months, forest structure characterization was done periodically during the period of study. For the comparative purpose of this work we have summarized and compiled different stand structure metrics measured along the study years (Table 3). Basal area (BA, m^2 ha^{-1}) and tree density (D, trees ha^{-1}) were estimated by measuring tree diameters at basal and breast heights ($D_{B,}$ and D_{BH} respectively, cm) and counting all trees in the plots. Diameter distribution was classified into 4 classes (CAL: D_{BH}<3.5 (1), 3.5≤ D_{BH}<7.5 (2), 7.5≤ D_{BH}<10.5 (3), D_{BH}≥10.5 (4); HU: D_{BH}<7.5 (1), 7.5≤ D_{BH}<11 (2), 11≤ D_{BH}<15 (3), D_{BH}≥15 (4), figures in cm). Forest cover (FC, %) was measured in all of the blocks with a vertical densitometer (GRS, USA) with 50 readings per block in a 3x3 m grid. Leaf Area Index (LAI, m^2 m^{-2}) was seasonally estimated in each block at 1.0 m above ground using a LAI-2000 sensor (LI-COR, 1991, LI-Cor Inc., Lincoln, NE, USA) as described in Molina and del Campo (2011) and Leblanc and Chen (2001). All measurements were made within areas at least 2 m away from the plot limits to avoid edge effects.

2.3. Rainfall partitioning: Pg, throughfall, stemflow and interception

The study spans the period from October 1, 2013 to September 30, 2016 in the Calderona site and from October 1, 2012 to September 30, 2016 in La Hunde site, giving a total of 3 and 4 water years respectively. In both sites, we set a central data-logging unit (CR1000, Campbell Sci., UT, USA) to register and store data, supplemented with two AM16/32B Multiplexers, two SDM-IO16 expansion modules, a solar panel and a 12V battery. The system was programmed to read the sensors output every 5 seconds or one minute and to record the values every 5 s, 10 min or 30 min, depending on the sensor and the environmental conditions, see text below.

Gross Precipitation (Pg) was characterized by considering its specific rain-related features (rainfall) and its meteorological characteristics (event-meteorology). Pg was continuously measured by means of a tipping-bucket rain gauge located over the canopy (6 m above ground), with 0.2-mm resolution (7852, Davis Instruments Corp., Hayward, CA, USA) and programmed to measure, when raining, at 5-sec intervals. To study the rainfall and the event-meteorology, all data were re-grouped into 10-min intervals, as this time lapse is more common in the literature. In the analysis of Pg, we used Modified Julian Days (MJD), which facilitated the tallying of daily totals, and allowed to compute the length of rain events simply by subtracting the starting and ending dates. In event-based studies of interception it is vital to report both, the minimum inter-event time and the resulting structure of intra-event gaps (Dunkerley, 2008). Minimum inter-event time was set to 1-hour, which ensures that two consecutive rainfall events come from different clouds (Llasat, 2001). According to this criterion, rain depth (Pg, mm), rain event duration (P_D, min), maximum and mean rain rate or intensity recorded during an event (P_I and P_{Imx}, mm/h) and intra-event gaps (as the proportion of the time within each event with no rainfall, P_{Gap}) were calculated. Only events over 1 mm were included in the analysis (Muzylo et al., 2012). Also, in order to identify the relative importance of convective high-intensity events, we adopted a threshold intensity of 50 mm/h (Llasat, 2001) corresponding to a time interval of 1-min. The increase of the time interval from 1-min to 10-min in our case provokes an attenuation of the high-intensity peaks, which in our case led to an equivalent reduced threshold intensity of 23.8 and 21.5 mm/h for CAL and HU sites, respectively (these thresholds are the 10-min equivalents to the 1-min 50 mm/h in our events sample). By using these thresholds we computed the $\beta_{23.8,10}$ and $\beta_{21.5,10}$ parameters for each event as an indicative of its convective nature (Llasat, 2001), with values of β=0 non-convective; 0<β≤0.3 slightly convective; 0.3<β≤0.8 moderately convective and 0.8<β≤1.0 strongly convective.

The variables used to characterize the event-meteorology were: mean and maximum wind speed (U_{av} and U_{mx}, 7911 anemometer, Davis Instruments Corp.), air temperature and relative humidity (T, RH sensor, Decagon Devices, Pullman, USA) and vapour pressure deficit (D). Sensors were placed close to the rainfall gauge on the same mast, at a height above canopy, recorded in the same time interval (5-sec when raining, 1-min averaged to ten minutes when no rain) and stored on the data logger.

Stemflow (Stf) was measured by sealing stem collars to 4/3 trees per diameter class per plot (n per treatment was between 9 and 16, as the treated plot in CAL had no trees belonging to the lower class). The bark on each sample tree was scraped off to smooth the surface in preparation for the fitting of a plastic collar with polyurethane sealant at a variable height between 0.3 and 1.2 m. After the plastic collars were attached, plastic tubes were inserted into small holes located in the lowest part of the collars to collect the water and divert it to tipping-buckets (Pronamic 100.054, 1 mm resolution, time lapse 10 min, 5-sec when raining) and then to 25 L deposits (10- to 15-day intervals, for validating). At tree scale, three key parameters (Levia and Germer, 2015) were considered, the stemflow volume (or yield) of an individual tree i (Stf_i, l tree^{-1}) for a given Pg_j event; the stemflow coefficient (or rate) of a tree ($CStf_i$, l tree^{-1} mm^{-1}), which is the quotient of the tree stemflow volume drained (Stf_i) to the amount of precipitation (Pg_j in mm) that caused it. The efficiency of an individual tree to produce stemflow on a unit of ground area (a proxy to the funneling ratio as defined in Herwitz, 1986) was computed by dividing $CStf_i$ over the tree crown projected area: $CStf_{i.m}{}^2 = CStf_i / CA_i$, where, $CStf_{i.m}{}^2$ is the specific stemflow coefficient of tree i (l mm^{-1} m^{-2}), and CA_i is the crown projected area of tree i (m^2).

Up-scaling to the equivalent stand-scale stemflow depth (mm) was performed by using the cover (FC) in the block as scalar (Swaffer et al., 2014). Due to extremely high tree density in one of the plots, up-scaling with density (Leiva and Germer, 2015) was discarded as it might produce overestimations. We found both $CStf_i$ and $Cstf_{i.m}{}^2$ varying as a function of tree size (D_B, D_{BH} and CA) with significant power functions ($Y=aX^b$, with Y either $CStf_i$ or $Cstf_{i.m}{}^2$ and X the tree size-related metric, $r^2>0.85$, n=18). Consequently, to obtain the stemflow depth per block, we used these power functions to obtain correction factors so that the measured stemflow for any Pg_j event corresponding to the mean *sampled tree* was corrected to the mean *block tree*. Accordingly, the stemflow depth per block was estimated as:

$Stf_{Bi,j}$ (l m^{-2}) = $CStf_m{}^2{}_{i,j}$ (l mm^{-1} m^{-2}) * Cf * Pg_j (mm) * Forest Cover (fraction)

Where $Stf_{Bi,j}$ is the ground-based stemflow depth of a Pg_j event in the block i (i=1,2,3, either for T or C), $CStf_m{}^2{}_{i,j}$ is the mean specific stemflow coefficient of sampled trees in the block i for that Pg_j event, Cf is the correction factor to adjust for the $CStf_{i\_m}{}^2$ of the mean tree in the block (with slightly different crown-projected area) and Pg_j j=1,..m the gross rainfall event. Finally, the rate of stemflow (%) for each block was considered as the ratio between $Stf_{Bi,j}$ and the gross rainfall depth Pg_j, multiplied by 100, as an efficiency index of the stand structure to channel the water that falls onto its canopy towards the soil.

Throughfall (Thr), was measured by setting out 15 (CAL) or 9 (HU) galvanized steel gutters per plot (5 or 3 per block according to the site), arranged following contour lines and maintained in the same positions throughout the study (Llorens et al., 1997). The devices were 200/250 cm long and 30.7/40 cm wide (CAL/HU), set at 50 cm above the soil and sloping towards water counters equipped with pulse counters (Altair V4, Diehl Metering, minimum flow rate 5 L/h). 25 L deposits gauged in 10-15 days intervals were additionally attached to the gutters in order to cross calibrate the whole system. Total collecting area per gutter was 0.613 (CAL) or 0.813 m^2 (HU), considered to be a suitable area to obtain an estimate of the mean with a 95% probability (Rodrigo and Avila, 2001). Although fixed rain gauges can lead to systematic errors and uncertainties (Lloyd and Marques, 1988), total sampled area in our case (between 7.3 and 9.2 m^2/plot, or about 0.27 rain gauges of 200 cm^2 per m^2) leads to errors less than 6% in throughfall (Lloyd and Marques, 1988) because large collectors integrate the throughfall from a broader canopy area and decreases the spatial variability. The time-lapse for the counters was 5-sec when raining or 10-min for no raining periods.

Event interception (It) depth (mm) and rate (%) were computed as the difference between gross rainfall minus the sum of throughfall and stemflow of that event. For the blocks' average, when this amount scored negative values, it was set to zero (as dripping points in some gutters should be offset by less throughfall in others).

2.4. Data treatment and analysis

Treatment effects were assessed by comparing T and C plots for event stemflow, throughfall and interception (mm), their respective rates to Pg (%) and the cumulative daily trends during the entire study period.

Data were quality-controlled for spikes and gaps. In some cases, larger data gaps were completed using meteorological data from nearby stations (Serra and Ayora-La Hunde from SAIH network) to estimate Pg and the meteorological variables, and then, simple linear regressions with Pg to estimate the additional variables for rainfall partitioning (stemflow and throughfall). When fitted models were not good enough or not appropriate, we used Artificial Neural Network (Multilayer Perceptron Network, MLP SPSS, IBM Corp., 2013) to estimate interception (mm) using forest structure and precipitation variables as predictors (correlation between predicted values and holdout sample was 0.95). All statistical proofs on the effect of thinning/clearing were performed considering only empirical data, i.e. data estimated to fill in gaps were exclusively used for computing accumulated temporal values.

Differences in depth and rates in Stf, Thr and It between T and C were analysed through an ANCOVA analysis considering treatment (C, T) and block (1-3) as factors and Pg as covariate (performed in SPSS, IBM Corp., 2013). In the case of Stf on a tree basis, an ANCOVA with D_B as covariate was performed. Data were examined for normality and homogeneity of variance (Levene's test), and observing the interaction term between the covariate and treatment tested homogeneity in the regression slopes. When these assumptions were violated, the variables were transformed with power functions to achieve homoscedasticity or, alternatively, a nonparametric Kruskal–Wallis test based on the chi-squared statistic was used. A significance level of $p<0.05$ was used for all analyses.

To study the relationships of rainfall, event-meteorology and forest structure on the response variables (Stf, Thr and It), boosted regression trees models (BRT) were performed in R software (R core team, 2015), using package ‘‘gbm” (Tanaka et al., 2015, 2017; Ridgeway, 2017; Elith and Leathwick, 2017; Zabret et al., 2018). In the BRT analysis, a Gaussian distribution family, a learning rate of 0.005, a tree complexity of 4-5, and a bag fraction of 0.75 were set. The minimum number of trees was in all cases above 1500. The results of this analysis provide the relative influence (RI) of the predictors on the response variable, which measures the number of times a predictor variable is selected for splitting, weighted by the squared improvement to the model as a result of each split, averaged over all trees, and scaled so that the sum adds to 100 (Elith et al., 2008). The higher the RI the stronger the influence of the predictor in the response variable. The RI for the most influential variables in the models was plotted in partial dependence plots (PDP) using the mentioned package in R software.

Cumulative treatment impacts on response variables (Stf, Thr and It) were evaluated in terms of a shift of the daily ratio of treated/control following the intervention: ln (T/C) (Perry and Jones, 2016). Because of the complete block design layout, we assumed baseline (in the pre-operational period) to be zero.

3. Results

3.1. P characteristics

Total Pg accumulated in the Calderona site (CAL) was 162, 370 and 246 mm for water years 13-14, 14-15 and 15-16 respectively. During the period spanning from September 1, 2013 to September 20, 2014, only 105 mm were recorded (the driest year on record for many meteorological stations in the region). As a consequence, since mid 2014 a generalized tree mortality and dieback was observed over the area. In La Hunde site (HU), measured Pg accumulated a total of 534, 271, 426 and 297 mm for the water years from 12-13 to 15-16 respectively. In general, non-convective rainfall events in HU presented higher Pg (1 mm more on average) and P_D (1.87 hours more on average) than in CAL (Table 4). On the contrary, this latter site presented higher P_I, P_{Imx} and P_{Gap} and higher evaporative atmospheric conditions (both D and U) reflecting a higher torrential pattern in the precipitation. In this sense, CAL also presented higher rainfall convectivity than HU, as observed in the higher relative number of events with $\beta \neq 0$ (8.7% of the events, 38% of Pg in CAL vs. 4.2% of the events and 11% of Pg in HU), and their higher values in Pg, P_D, P_I, P_{Imx} and atmospheric turbulence (U) and water vapour demand (D) (Table 4, $\beta \neq 0$). β presented maximum values of 0.91 in CAL (44 mm, 98 minutes) and 0.75 in HU (31 mm, 80 minutes)

3.2. Stemflow on a tree basis

Stemflow at the tree scale was studied for events > 1mm for Stf, CStf and $CStf_{m^2}$. In CAL, the ANCOVA indicated no significant differences between T and C either in Stf nor CStf (Table 5). On the contrary, $CStf_{m^2}$ showed a significant difference between both treatments (Table 5, Figure 2), indicating that treated trees were less efficient when funnelling water with respect their crown-projected area. In this site, the mean sampled tree for stemflow presented a D_B of 10.96 and 12.88 cm in C and T, respectively, and a crown-projected area of 3.15 and 5.67 m^2 in C and T, respectively.

In HU site, Stf and CStf had to be analyzed through a Kruskal-Wallis test sorting the data by diameter class. There were differences between C and T only for the bigger trees in Stf and CStf (Table 5, Figure 2). Regarding $CStf_{m^2}$, the ANCOVA (D_B covariate) also indicated significant differences between the treatments, with higher value for T (Table 5, Figure 2). In this site the mean sampled tree for stemflow presented a D_{BH} of 10.9 and 14.14 cm in C and T, respectively, and a crown-projected area of 7.1 and 8.1 m^2 in C and T, respectively.

3.3. Event throughfall, stemflow and interception

In both sites, the throughfall per event was significantly higher in T than in C (Table 5, Figure 3) in both depth and rate, according to the ANCOVA test. On the contrary, interception was significantly lower in T than in C in both sites for depth and rate (Table 5, Figure 3). In CAL site, event stemflow on a ground basis was higher in C than in T for both depth and rate according to the Kruskal-Wallis test (Table 5, Figure 3). In HU, event stemflow on a ground basis was no different between treatments (Table 5, Figure 3).

3.4. Influence of rainfall features and forest structure on rainfall partitioning

In both sites, rainfall characteristics and forest structure were used as predictors of the different variables of rainfall partitioning (Table 6; Figures 4 and S3) by using BRT models. Cross-validation correlation coefficients presented better score in depth-expressed (mm) variables, ranging between 0.824 and 0.993, than in rates (% Pg), ranging between 0.434 and 0.947 (Table 6). The analyses of relative influence (RI) performed through BRT, sorted the impact of the different independent variables on the response variables. It is remarkable from Table 6 and Figures 4 and S3 the overwhelming importance of the rainfall variables of the event (Pg, P_D, $P_{I,}$ $P_{Imx,}$ P_{Gap} and β) on the amount (mm) of Stf, Thr and It, with a weighted RI of 77% (overall models). On the contrary, the contribution of these variables to the rates was modest regardless of the site (RI~16%). Forest structure and the meteorological conditions during rainfall scored an RI less than 20% in the depths, but their RI in the rates increased up to 38 and 26% respectively in the overall models (Figure 4). In the drier pine site, rainfall partitioning (either depth or rate) was more affected by forest structure and event-meteorology (39 and 29% in rates respectively) than in the moister oak site (9 and 25% in rates respectively), although in this latter site (HU), event-meteorology scored the highest RI for rates compared with forest structure and rainfall features. It should be stressed that the models fitted for the drier site of CAL explained more variation than those fitted in HU.

Averaging over the whole period in both plots, simple regression fitted between It rates and forest structure, yielded better fit for LAI (r^2=0.83) than for canopy cover (r^2=0.68) (Figure 5).

3.5. Cumulative interception and temporal trends

Interception was always lower in T than in C in both sites (Figure 6) through the study period, with total accumulated values of It in CAL of 153.4 and 229.0 mm for T and C plots, respectively, out of a total Pg of 779 mm. By water years (Figure 6), 13-14 was the driest (162 mm), registering 24.0 and 29.6% of It in T and C plots, respectively. These percentages diminished in 14-15 to 19.4 and 27.8% for C and T plots respectively, while in 15-16 the values were 16.7 and 31.7% for C and T, respectively. In HU site, T and C plots intercepted a total amount of 234.2 and 440.8 mm respectively out of a total Pg of 1501.4 mm during the four water years analyzed. By water years (Figure 6), T and C percentages were respectively 12-13: 31.7 and 11.4%; 13-14: 29.0 and 16.0%; 14-15: 27.7 and 18.0%; 15-16: 25.3 and 17.2%. These values are slightly different to those reported in the event-based analysis as most events with Pg< 1 mm were considered as fully intercepted.

The temporal trend observed in Figure 7 shows that the differences between C and T in both sites were hold during the span considered (3 and 4 years in CAL and HU respectively). Nevertheless, the temporal changes in magnitude differed between sites: whilst in HU the differences in Stf, Thf and It are diminishing with the elapsed time since clearing, in CAL there is a more static pattern with even slight increments along time in the differences between C and T plots for both It and Thr. In HU, wet periods from water year 13-14 onwards made the ratio ln T/C to decrease, whilst dry interims tend to hold the differences (flattening the series). In the It series, the ratio changed from -0.9 (2013) to -0.6 (2016). On the other hand, in CAL, light and sparse rainfall events dominated over the whole period without a marked wet season, making the differences to persist and slightly increase along time: It ratio changed from -0.30 to -0.38 between the beginning and the end of the studied period.

4. Discussion

Rainfall features showed a contrasted pattern between both sites, reflecting the different meteorological and climatic characteristics. In CAL site, the proximity to the Mediterranean Sea clearly influenced the higher convectivity, dryness and warmth as compared to HU site, despite the difference in altitude between both sites was only 200 m. In CAL, wet periods are almost absent, and important rainfall events (e.g. Pg>10mm) are sparse and scattered along the year, mainly associated to convective rainfall. On the contrary, in the cooler inland site, HU, wet periods do occur and significant precipitation can accumulate in just a few days, as rain events may concatenate during consecutive days. Considering a threshold of 2 mm h^{-1} for mean rainfall intensity to separate low (L) and high (H) intensity events (Muzylo et al., 2012) and a 5-hour rainfall duration threshold to distinguish short (S) and long (L) rainfall events (Llasat, 2001), we may classify the rainfall as low/high intensities and short/long durations (L/S, L/L, H/S and H/L; Table S1, supplementary material). Whilst H/L events had a similar low frequency in both sites (about 2-3%), the remaining classes were very irregularly distributed, with relative frequencies of 52% and 25% in H/S, 3% and 17% in L/L and 41% and 56% in L/S for CAL and HU respectively. Total Pg in each class is presented in Table S1, supplementary material. These figures are in turn different in a site among different water years, reflecting an accused inter-annual variability. For instance, in CAL, the extremely dry year 13-14, registered 87% of total Pg as H/S.

The marked differences in the combined meteorological features of Pg had a primary role in rainfall partitioning. Regardless of the treatment, mean Pg event-based interception loss was 1.16 mm (24.6%) and 0.90 mm (18.9%) for CAL and HU respectively, being the rate higher in H/S events and the depth in H/L (Table S2), as previously reported by Muzylo et al., 2012.

At the tree-scale, stemflow yield was proportional to tree size and only bigger oaks (D_{BH} classes 3 and 4) were significantly affected by the treatment, with higher Stf and CStf than their relatives in the control plot. Stemflow yield is directly related to the 3-dimensional geometry of the crown (Levia and Frost, 2003) and higher crown densification was observed in the cleared oaks, especially in the top diameter classes (e.g. LAI under the trees was 0.81 and 0.93 in the control and treated plots respectively, unpublished data). This indicates that the crown structure changed after the treatment in a fashion that improved both, the amount and the efficiency, by which the water is funneled onto the trunk towards the soil. This differential impact of thinning on growth depending on tree size has been previously reported in holm oak (Mayor and Rodà, 1993).

However, the significant enhancement of the stemflow at tree scale resulted in no differences at the ground scale, due to the effect of thinning on density: higher stemflow per tree was counterbalanced with a lower number of trees, so the role of forest structure on this flux was essentially absent (Table 6). In this site, it stands out the very low yields of stemflow observed at the ground scale (<1% Pg), which contrast with the higher amounts (> 6% Pg) previously reported for the species in the Mediterranean

(Bellot and Escarré, 1998; Llorens and Domingo, 2007; Limousin et al., 2008). The particular spatial forest structure of our low-biomass forest is responsible for these differences. For instance, in the work of Limousin et al. (2008) control and thinned plots have 5464 and 2364 trees ha^{-1} respectively (1155 and 310 trees ha^{-1} in this study) and LAI values between 3.1 and 1.6 m^2 m^{-2} (1.1-0.6 m^2 m^{-2} in our case). Other studies with low-density stands of holm oak also reported negligible stemflow yields (Mateos and Schnabel, 2001; Hassan et al., 2017). On a tree scale, our data are much closer to the values reported elsewhere (Bellot and Escarré, 1998). The plagiotropic habit of growth, the roughness of the bark, or the trunk storage capacity (Zabret et al., 2018) are likely responsible for the low values of Stf in this species.

Stemflow yield per pine (in CAL site) was higher than in the oaks. Lower tree size (less surface on which collect and store water), lower bark water storage capacity (smooth at their early ages) and steeper branch inclination angles, are known to be key factors controlling stemflow volumes (Levia and Frost, 2003; Levia and Germer, 2015). However, there is a threshold where less projected crown area offsets the steeper angles and stemflow yields decline. Not only tree structure but also rainfall differences between both sites may have contributed to the differences in stemflow production. Convective storms with high intensity may result in a larger stemflow flux than rainfall associated to fronts (Dunkerley, 2014). This author found that the temporal variation of rainfall intensity and higher peak rainfall intensities yielded larger stemflow volume than events with constant intensity. Regarding the treatment, even though both Stf and CStf were slightly higher (non-significant) in the thinned trees, the funneling ratio ($CStf_{m^2}$) was significantly higher in the control. Higher crown opening, development and exposure in the treatment may have increased the probability of both crown evaporation and branch drip and thus decrease stemflow efficiency by decreasing branch inclination angle, overloading preferential flow paths on trunks and forcing stemflow to become throughfall (Crockford and Richardson, 2000; Levia and Germer, 2015). Also, isolated trees in the treatment are more exposed to crown evaporation and, in fact, BRT models brought out in the event-meteorology a RI of 29% in the stemflow rate (16% in depth) in this site. Regarding forest structure, the BRT model assigned a RI of 58% of the total observed variation in stemflow rate (7 % in mm), well above the values in the HU site, suggesting that changes in forest structure are more important when meteorology becomes more evaporative. BRT models can help to disentangle and rank the complicated influences on stemflow (Tanaka et al., 2017). Pine density and diameter distribution after the treatment had a profound and significant effect on the stemflow depth (mm): T plot presents similar range to that reported in the species (Llorens and Domingo, 2007; Molina and del Campo, 2012) whereas C reached higher values, close to 10% of Pg, which is consequence of the high tree density and cover (Levia and Frost, 2003). As a localized point of water input, stemflow must necessary increase at the expense of throughfall when the number of trees increases and the volumes of water funneled down the tree trunk are significant (Dunkerley, 2014). In this case, as stemflow depth was negatively affected by the thinning, opposite assessments may arise according to the pursued effects of the treatment (hydrological, eco-hydrological or hydro-geomorphological) as stemflow has proven influences on preferential and subsurface flows, soil moisture patterns, localized deep drainage hot spots, subsurface tunnel erosion, retreat of gullies etc. (see Leiva and Germer, 2015 for references).

Regarding throughfall and interception, both depth and rate were significantly affected by the treatment during the following years in both sites, as expected (Crockford and Richardson, 1990; Bréda et al., 1995; McJannet and Vertessy, 2001; del Campo et al., 2014). Thr and It in Mediterranean forests and scrublands are variable according to the forest species/structure and the rainfall features (Mateos and Schnabel, 2001; Llorens and Domingo, 2007; Muzylo et al., 2012; Swaffer et al., 2014). Although our data fit into those general ranges, a detailed analysis is needed in order to better address the specific effects of this adaptive silviculture in low-biomass stands. In Holm oak, Thr and It fractions in our control plot (about 69% and 28% of Pg respectively) are in the range compiled for this species (57-72 % and 18-31% of Pg for Thr and It respectively, see Limousin et al., 2008 and references therein). However our forest structure is quite simpler (LAI, cover and BA are much lower in our site) and that may lead to think that our It values are high when compared with structures having higher canopy storage capacities. In the cited work, their thinned oak plot had a similar cover to that in our control plot (~60%) and evaporated around 20% of Pg, pointing out that It was indeed higher in our drier conditions. The important difference is that, comparatively, these authors reduced It by 34% after removing 33% of BA, whereas in this work It was reduced by 60% after removing 41% of BA, indicating a higher relative gain in net precipitation, and that the evaporation did not decrease linearly in proportion to canopy structure with regards other forests of Holm oak (Gash et al., 1999; Limousin et al., 2008). Other studies with isolated trees and canopy cover around 20% or less (Mateos and Schnabel, 2001; Pereira et al 2009b; Hassan et al., 2017) reported It values below 10% of Pg, which agree with our experimental fit in Figure 5, and confirm higher It values under dry Mediterranean conditions. Regarding the pine saplings in CAL site, similar assertions can be made: It rates are in the reported range for this species and/or for similar climatic conditions (Crockford and Richardson, 1990; Llorens and Domingo, 2007; Shachnovich et al., 2008; Molina and del Campo, 2012; Swaffer et al., 2014) in spite their lower biomass. However the effect of thinning in our case had a greater relative effect on It reduction: a removal of 13 m^2 ha^{-1} of BA, decreased It by 46% (or 15% less intercepted Pg, i.e. -1.28% per unit of BA removed). Previous work in mature Aleppo pine trees achieved reductions -0.86% per unit of BA removed (Molina and del Campo, 2012) (Figure 8). For other species and climates, our data stand out for being out of range when relating It to forest structure either as It/LAI or It/BA ratios (Crockford and Richardson, 2000). Therefore, a reduction of forest structure in low-biomass unmanaged forests can produce a proportional greater effect in net precipitation than a comparable reduction in more stocked and mature forests (Figure 8). Thinning 40% of BA in holm oak has been stressed as the best managing option for enhancing disturbance resilience in this species (López et al., 2009).

Both the evaporative conditions and forest structure of our low-biomass forests explain these differences with previous thinning studies. In most experiments, thinning represents a shift from a closed-canopy control, where exponential eddy and wind speed decay can be assumed, towards a more opened and ventilated forest structure, where overall aerodynamic conductance and evaporation rates on wet isolated trees depends mostly on the surrounding, rather than on above-canopy environmental conditions (Pereira et al., 2009a). This means that reduced It in the control can be partially offset by enhanced evaporation resulting from higher aerodynamic conductance due to higher wind speed and more effective turbulent mixing (Teklehaimanot et al., 1991; Pereira et al., 2016). In our case, however, low forest cover and sparseness were already present in the controls (79 and 63% of cover in CAL and HU respectively), so the impact of thinning on increasing turbulence and wind speed at the tree crowns level was comparatively lower than in other studies. Decoupling coefficients (Jarvis and McNaughton, 1986) calculated for the oaks (unpublished data) were below 0.1 for C and T respectively, indicating a high degree of coupling between the canopy and the free air stream regardless of the treatment. Similar rationale was provided in Crockford and Richardson (2000) to explain the high interception in a low-cover pine plantation. Also, it can be argued that the relative gain in net precipitation (or efficiency of the thinning) in CAL was somewhat lower than in HU (Figure 8) due to the important contribution of meteorology during rainfall in the former site, which actually weighted more than in the latter site in the BRT fitted (Table 6). Likewise, the control trees in CAL site (third block, Table 3), can behave as a closed canopy forest (Pereira et al., 2016), and thus a lower depth of the fully ventilated part of the canopy makes the upper part of the crown the main contributor to evaporation (the above-mentioned offsetting effect would have been greater in this case). These findings underscore the importance of rainfall evaporative conditions in semiarid climates (Dunkerley, 2000; Llorens et al., 1997) together with their relationship to forest structure (Pereira et al., 2016) and suggest again the higher relative importance of forest structure in rainfall partitioning when the evaporative conditions are enhanced (Table 6 and Figure 4). Along time, the effects of the thinning are dampening in HU as a consequence of the growth of crowns in the treated trees (del Campo et al., 2014), which can also be argued as a reason for the lower importance of forest structure in this site, as it was considered constant through time. López et al., (2003) reported a lag of the response to thinning for fine roots growth of about 1.5 years, a span that in our case would explain why during the first year after clearing the differences (ln T/C) peaked and decreased thereafter. Higher net precipitation, soil temperature and soil nutrient content (from mulch mineralization in thinned plot, unpublished data) enhance tree growth (López et al., 2003). However, converging C and T values was not just due to increasing It in T, but to decreasing It in C too. During the 4-years period we measured decreasing LAI and transpiration values in C due to leaf abscission (unpublished data), a response of this species to severe droughts in order to decrease stand It and allow improved soil moisture (Barbeta and Peñuelas, 2016). This underscores the importance of these adaptive water-oriented treatments and encourages future monitoring of this temporal trend. Holm oak forests have shown climate-related mortality and growth decline since the last century (Camarero et al., 2016), and years 2014 and 2015 presented in this site very low precipitation and high temperatures that may push marginal populations close to their distributional limit (Peñuelas et al., 2017). On the other hand, in CAL, dryness and lack of enough wet years led to no temporal drift on ln T/C, and thus a longer duration of the effects of treatment due to low growth rates.

6. Conclusions

The results presented in this paper highlight that interception loss in low-biomass semiarid forests is comparable or even higher to that of mature forests of the same species with higher storage capacity but similar forest cover. Accordingly, the effectiveness of a proactive-adaptive silviculture aimed to increase net rainfall has been shown to be comparatively higher in terms of water quantity but also it is more cost-effective, due to the removal of less biomass per unit of area treated. The impact of forest structure modification on rainfall partitioning seems to be related to the dryness of the site. In the RI analysis, event-meteorology and forest structure were more important in the drier site of Calderona (comparing between sites), although in an intra-site comparison, event-meteorology was more important than forest structure in La Hunde and the opposite was true in Calderona. The temporal effect of the treatments on tree growth might explain the weaker RI of forest structure in rainfall partitioning in La Hunde, where growth dynamics likely dampened the differences along time. In the case of the drier climate, the temporal effects of thinning appear to last longer than in the wetter site due to a slower growth response of the remaining trees following severe droughty years.

This study can make a contribution towards the implementation of ecohydrological-oriented silviculture in semiarid regions by explicitly addressing issues related to the magnitude, efficiency and duration of the effects of treatments in these stands on net rainfall. Evaporation components between events and in dry spells (transpiration, soil and litter evaporation, etc.) as well as the redistribution of infiltrated water must be further addressed in order to have a full picture of the efficiency of treatments in terms of blue and green water balance. Also, additional water years are needed in order to better know about the temporal dynamics of these effects and define time interims for successive forest treatments.

Acknowledgements

This study is a component of research projects: HYDROSIL (CGL2011-28776-C02-02), SILWAMED (CGL2014-58127-C3-2) and CEHYRFO-MED (CGL2017-86839-C3-2-R) funded by the Spanish Ministry of Science and Innovation and FEDER funds. The authors are grateful to the Valencia Regional Government (CMAAUV, Generalitat Valenciana), VAERSA and ACCIONA for their support in allowing the use of the experimental forest and for their assistance in carrying out the fieldwork.

References

Allen, C.D., Breshears, D.D., McDowell, N.G., 2015. On underestimation of global vulnerability to tree mortality and forest die-off from hotter drought in the Anthropocene. Ecosphere 6, 1–55.

Barbeta, A., Peñuelas, J., 2016. Sequence of plant responses to droughts of different timescales: lessons from holm oak (*Quercus ilex*) forests. Plant Ecol. Diver. 9(4), 321-338.

Bellot, J., Escarré, A., 1998. Stemflow and throughfall determination in resprouted Mediterranean holm-oak forest. Ann. For. Sci. 55(7), 847–865.

Bréda, N., Granier, A., Aussenac, G., 1995. Effects of thinning on soil and tree water relations, transpiration and growth in an oak forest (Quercus petraea (Matt.) Liebl.), 1995. Tree Physiol. 15 (5), 295-306.

Camarero, J.J., Sanguesa-Barreda, G., Vergarechea, M., 2016. Prior height, growth, and wood anat- omy differently predispose to drought induced dieback in two Mediterranean oak species. Ann. For. Sci. 73, 341-351.

Carlyle-Moses, D.E., 2004. Throughfall, stemflow, and canopy interception loss fluxes in a semi-arid Sierra Madre Oriental matorral community. J. Arid Environ. 58, 181–202. doi:10.1016/S0140-1963(03)00125-3

Crockford, R. H., Richardson, D.P., 1990. Partitioning of rainfall in a eucalypt forest and pine plantation in southeastern Australia: IV. The relationship of interception and canopy storage capacity, the interception of these forests, and the effect on interception of thinning the pine plantation. Hydrol Process. 4(2), 169-198.

Crockford, R.H., Richardson, D.P., 2000. Partitioning of rainfall into throughfall, stemflow and interception: effect of forest type, ground cover and climate. Hydrol Process. 14, 2903-2920.

del Campo, A.D., Fernandes, T.J.G., Molina, A.J., 2014. Hydrology-oriented (adaptive) silviculture in a semiarid pine plantation: How much can be modified the water cycle through forest management?. Eur. J. Forest. Res., 133(5), 879-894.

del Campo, A.D., González-Sanchis, M., Lidón,A., García Prats, A., Lull, C., Bautista, I., Ruiz, G., Francés, F., 2017. Ecohydrological-Based Forest Management in Semi-arid Climate, in: Křeček, J., Haigh, M., Hofer, T., Kubin, E., Promper, C. (Eds.), Ecosystem Services of Headwater Catchments. Co-published by Springer Int. Publishing, Switzerland, with Capital Publishing Co., India, pp. 45-57.

Doblas-Miranda, E., Alonso, R., Arnan, X., Bermejo,V., Brotons, L., de las Heras, J., Estiarte, M., Hódar, J.A., Llorens, P., Lloret, F., López-Serrano, F.R., Martínez-Vilalta, J., Moya, D., Peñuelas, J., Pino, J., Rodrigo, A., Roura-Pascual, N., Valladares, F., Vilà, M., Zamora, R., Retana, J., 2017. A review of the combination among global change factors in forests, shrublands and pastures of the Mediterranean Region: Beyond drought effects. Glob. Planet. Change 148, 42-54.

Dunkerley, D., 2000. Measuring interception loss and canopy storage in dryland vegetation: a brief review and evaluation of available research strategies. Hydrol. Process. 14, 669–678.

Dunkerley, D., 2008. Identifying individual rain events from pluviograph records: a review with analysis of data from an Australian dryland site. Hydrol. Process. 22, 5024–5036.

Dunkerley, D., 2014. Stemflow on the woody parts of plants: Dependence on rainfall intensity and event profile from laboratory simulations. Hydrol. Process. 28(22), 5469–5482.

Elith, J., Leathwick, J.R., Hastie, T., 2008. A working guide to boosted regression trees. J Anim Ecol. 77(4), 802–813.

Elith J., Leathwick J., 2017. Boosted regression trees for ecological modelling. 22pp. http://cran.r-project.org/web/packages/dismo/vignettes/brt.pdf (accessed 10.05.2018)

Fernandes, T. J., del Campo, A. D., Herrera, R., Molina, A. J., 2016. Simultaneous assessment, through sap flow and stable isotopes, of water use efficiency (WUE) in thinned pines shows improvement in growth, tree-climate sensitivity and WUE, but not in WUEi. For. Ecol. Manag. 361, 298-308.

García de la Serrana, R., Vilagrosa, A., Alloza, J. A., 2015. Pine mortality in southeast Spain after an extreme dry and warm year: interactions among drought stress, carbohydrates and bark beetle attack. Trees 29, 1791-1804.

García-Prats, A., del Campo, A., Fernandes, T.J.G., Molina, A. 2015. Development of a Keetch and Byram-based drought index sensitive to forest management in Mediterranean conditions. Agric. For. Meteorol. 205, 40-50.

Gash, J.H.C., Valente, F., David, J.S., 1999. Estimates and measurements of evaporation from wet, sparse pine forest in Portugal. Agric. For. Meteorol. 94(2), 149–158.

Ganatsios, H.P., Tsiorasb, P.A., Pavlidisa, T., 2010. Water yield changes as a result of silvicultural treatments in an oak ecosystem. For. Ecol. Manage. 260(8), 1367– 1374.

González-Sanchis, M., del Campo A., Molina, A.J., Fernandes, T.J.G., 2015. Modeling adaptive forest management of a semi-arid Mediterranean Aleppo pine plantation. Ecol. Model. 308, 34–44.

Grant, G.E., Tague, C.L., Allen, C.D., 2013. Watering the forest for the trees: an emerging priority for managing water in forest landscapes. Front. Ecol. Environ. 11(6), 314–321.

Hassan S.M.T., Ghimire, C.P., Lubczynski, M.W., 2017. Remote sensing upscaling of interception loss from isolated oaks: Sardon catchment case study, Spain. J. Hydrol. 555, 489–505.

Herwitz, S.R., 1986. Infiltration-excess caused by stemflow in a cyclone-prone tropical rainforest. Earth Surf. Process. Landf. 11, 401-412.

IBM Corp. Released 2013. IBM SPSS Statistics for Windows, Version 22.0. Armonk, NY: IBM Corp.

Ilstedt, U., Bargués Tobella, A., Bazié, H.R., Bayala, J., Verbeeten, E., Nyberg, G., Sanou, J., Benegas, L., Murdiyarso, D., Laudon, H., Sheil, D., Malmer, A., 2016. Intermediate tree cover can maximize groundwater recharge in the seasonally dry tropics. Sci. Rep. 6, 21930.

Jarvis, P., McNaughton, K., 1986. Stomatal control of transpiration: scaling up from leaf to region. Adv. Ecol. Res. 15, 1-49.

Klein, T., Shpringer, I., Fikler, B., Elbaz, G., Cohen, S., Yakir, Y., 2013. Relationships between stomatal regulation, water-use, and water-use efficiency of two coexisting key Mediterranean tree species. For. Ecol. Manag. 302, 34–42.

Leblanc, S.G., Chen, J. M., 2001. A practical scheme for correcting multiple scattering effects on optical LAI measurements. Agric. Forest Meterol.110, 125– 139.

Levia, D. F., Frost E.E., 2003. A review and evaluation of stemflow literature in the hydrologic and biogeochemical cycles of forested and agricultural ecosystems, J. Hydrol. 274(1–4), 1–29.

Levia, D. F., Germer, S., 2015. A review of stemflow generation dynamics and stemflow-environment interactions in forests and shrublands. Rev. Geophys. 53, 673–714.

LI-COR, 1991. LAI-2000 Plant Canopy Analyser Operating Manual. Lincoln, Nebraska, EE.UU. LI-COR Inc.

Limousin, J.M., Rambal, S., Ourcival, J.M., Joffre, R., 2008. Modelling rainfall interception in a mediterranean Quercus ilex ecosystem: Lesson from a throughfall exclusion experiment. J. Hydrol. 357, 57-66.

Lindner, M., Fitzgerald, J. B., Zimmermann, N., Reyer, C., Delzon, S., van der Maaten, E., Schelhaas, M. J., Lasch, P., Eggers, J., van der Maaten-Theunissen, M., Suckow, F. Psomas, A., Poulter, B., Hanewinkel, M., 2014. Climate change and European forests: what do we know, what are the uncertainties, and what are the implications for forest management? J. Environ. Manage. 146, 69-83.

Llasat, M.C., 2001. An objective classification of rainfall events on the basis of their convective features: application to rainfall intensity in the northeast of Spain. Int. J. Climatol. 21, 1385–1400.

Llorens, P., Poch, R., Latron, J., Gallart, F., 1997. Rainfall interception by a Pinus sylvestris forest patch overgrown in a Mediterranean mountainous abandoned area I. Monitoring design and results down to the event scale. J. Hydrol. 199, 331-345.

Llorens, P., Domingo, F., 2007. Rainfall partitioning by vegetation under Mediterranean conditions. A review of studies in Europe. J. Hydrol. 335, 37– 54.

Lloyd, C.R., Marques, A. De O., 1988. Spatial variability of throughfall and stemflow measurements in Amazonian rainforest. Agricultural & Forest Meteo. 42(1), 63-73.

López, B.C., Sabaté, S., Gracia, C.A., 2003. Thinning effects on carbon allocation to fine roots in a Quercus ilex forest. Tree Physiol. 23, 1217–1224.

López, B.C., Gracia, C.A., Sabaté, S., Keenan, T., 2009. Assessing the resilience of Mediterranean holm oaks to disturbances using selective thinning. Acta Oecol. 35, 849–854.

Mateos, B., Schnabel, S., 2001. Rainfall interception by holm oaks in Mediterranean open woodland. Cuadernos de Investigación Geográfica 27, 27-38.

Mayor, X., Rodà, F., 1993. Growth response of holm oak (Quercus ilex L) to commercial thinning in the Montseny mountains (NE Spain). Ann. For. Sci. 50, 247-256.

McJannet, D., Vertessy, R., 2001. Effects of thinning on wood production, leaf area index, transpiration and canopy interception of a plantation subject to drought. Tree Physiol. 21, 1001–1008.

(dataset) Ministerio de Agricultura y Pesca, Alimentación y Medio Ambiente. Sistema automático de información hidrológica (SAIH). http://saih.chj.es/chj/saih/glayer?t=p

Molina, A., del Campo, A.D., 2011. Leaf area index estimation in a pine plantation with LAI-2000 under direct sunlight conditions: relationship with inventory and hydrologic variables. For. Syst. 20 (1), 108-121.

Molina, A., del Campo, A.D., 2012. The effects of experimental thinning on throughfall and stemflow: a contribution towards hydrology-oriented silviculture in Aleppo pine plantations. For. Ecol. Manage. 269, 206–213.

Muzylo, A., Llorens, P., Domingo, F., 2012. Rainfall partitioning in a deciduous forest plot in leafed and leafless periods. Ecohydrology 5(6), 759–767.

Pan, Y., Birdsey, R.A., Phillips, O.L., Jackson, R.B., 2013. The Structure, Distribution, and Biomass of the World's Forests. Annu. Rev. Ecol. Evol. Syst. 44, 593–622.

Peñuelas, J., Sardans, J., Filella, I., Estiarte, M., Llusià, J., Ogaya, R., Carnicer, J., Bartrons, M., Rivas-Ubach, A., Grau, O., Peguero, G., Margalef, O., Pla-Rabés, S., Stefanescu, C., Asensio, D., Preece, C., Liu, L., Verger, A., Rico, L., Barbeta, A., Achotegui-Castells, A., Gargallo-Garriga, A., Sperlich, D., Farré-Armengol, G., Fernández-Martínez, M., Liu, D., Zhang, C., Urbina, I., Camino, M., Vives, M., Nadal-Sala, D., Sabaté, S., Gracia, C., Terradas, J., 2017. Assessment of the impacts of climate change on Mediterranean terrestrial ecosystems based on data from field experiments and long-term monitored field gradients in Catalonia. Environ. Exp. Bot., https://doi.org/10.1016/j.envexpbot.2017.05.012

Pereira, F.L., Gash, J.H.C., David, J.S., Valente, F., 2009a. Evaporation of intercepted rainfall from isolated evergreen oak trees: do the crowns behave as wet bulbs? Agric. For. Meteorol. 149(3–4), 667–679.

Pereira, F.L., Gash, J.H.C., David, J.S., David, T.S., Monteiro, P.R., Valente, F., 2009b. Modelling interception loss from evergreen oak Mediterranean savannas. Application of a tree-based modelling approach. Agric. For. Meteorol. 149, 680–688.

Pereira, F.L., Valente, F., David, J.S., Jackson, N., Minunno, F., Gash, J.H., 2016. Rainfall interception modelling: Is the wet bulb approach adequate to estimate mean evaporation rate from wet/saturated canopies in all forest types? J. Hydrol. 534: 606–615.

Perry, T. D., Jones, J. A., 2016. Summer streamflow deficits from regenerating Douglas-fir forest in the Pacific Northwest, USA. Ecohydrology, https://doi.org/10.1002/eco.1790

R Core Team, 2015. R: A language and environment for statistical computing. R Foundation for Statistical Computing, Vienna, Austria. http://www.R-project. org/ (accessed 10.05.2018).

Ridgeway, G., 2017. Generalized Boosted Regression Models. https://cran.r-project.org/web/packages/gbm/gbm.pdf (accessed 10.05.2018).

Rodrigo, A., Avila, A., 2001. Influence of sampling size in the estimation of mean throughfall in two Mediterranean Holm forests. J. Hydrol. 243, 216-227.

Schmithüsen, F., 2013. Three hundred years of applied sustainability in forestry. Unasylva 240 (64 2013/1), 3-13.

Seidl, R., Spies, T. A., Peterson, D. L., Stephens, S. L., Hicke, J. A., 2016. Searching for resilience: addressing the impacts of changing disturbance regimes on forest ecosystem services. J. Appl. Ecol. 53, 120–129.

Shachnovich, Y., Berliner, P.R., Bar, P., 2008. Rainfall interception and spatial distribution of throughfall in a pine forest planted in an arid zone. J. Hydrol. 349, 168-177.

Swaffer B. A, Holland K. L, Doody T. M, Hutson J., 2014. Rainfall partitioning, tree form and measurement scale: a comparison of two co-occurring, morphologically distinct tree species in a semi-arid environment. Ecohydrology 7, 1331–1344.

Tanaka, N., Levia, D., Igarashi, Y., Nanko, K., Yoshifuji, N., Tanaka, K., Tantasirin, C., Suzuki, M., Kumagai, T., 2015. Throughfall under a teak plantation in Thailand: a multifactorial analysis on the effects of canopy phenology and meteorological conditions. Int. J. Biometeorol. 59, 1145–1156.

Tanaka, N., Levia, D., Igarashi, Y., Yoshifuji, N., Tanaka, K., Tantasirin, C., Nanko, K., Suzuki, M., Kumagai, T., 2017. What factors are most influential in governing stemflow production from plantation-grown teak trees? J. Hydrol. 544, 10-20.

Teklehaimanot, Z., Jarvis, P.G., Ledger, D.C., 1991. Rainfall interception and boundary layer conductance in relation to tree spacing. J. Hydrol. 123, 261–278.

Terradas, J., Savè, R., 1992. The influence of summer and winter water relationships on the distribution of Quercus ilex L. Vegetatio 99(100), 137-145.

UN, United Nations, 2017. United Nations Strategic Plan for Forests 2017–2030. http://www.un.org/esa/forests/documents/un-strategic-plan-for-forests-2030/index.html (accessed 21.01.18).

Ungar, E.D., Rotenberg, E., Raz-Yaseef, N., Cohen, S., Yakir, D., Schiller, G., 2013. Transpiration and annual water balance of Aleppo pine in a semiarid region: implications for forest management. For. Ecol. Manag. 298, 39–51.

Valbuena, P., del Peso, C., Bravo, F., 2008. Stand Density Management Diagrams for two Mediterranean pine species in Eastern Spain. Invest. Agr.: Sis. Recur. For. 17(2), 97-104.

Whitehead, D. and Kelliher, F.M., 1991. A canopy water balance model for a Pinus radiata stand before and after thinning. Agric. For. Meteorol., 55:109-126

Zabret, K., Rakovec, J., Šraj, M., 2018. Influence of meteorological variables on rainfall partitioning for deciduous and coniferous tree species in urban area. J. Hydrol. 558, 29-41.

TABLE CAPTIONS

Table 1. Selected published literature about rainfall partitioning. Shaded cells correspond to works with common points to the present study; by columns: 1) semiarid, dry or Mediterranean climate, 2) short to mid-term period studied (>=3 years), 3) low-biomass overstocked/unmanaged forests, 4) address the relative influence of rainfall characteristics, meteorological conditions and forest structure, and 5) explicitly considering the effect of forest management treatments. Abbreviations: P, mean annual precipitation (mm); T, mean annual temperature (ºC); D, tree density (trees ha^{-1}), BA, basal area (m^2 ha^{-1}); LAI: leaf area index (m^2 m^{-2}); P-ev, event rainfall characteristics; P-met, event meteorological characteristics; FS, forest structure.

Table 2. Physiographic, climatic and edaphic features in both experimental sites (Calderona, CAL and Hunde, HU) and plots (0, control, not treated and 1, treated cleared/thinned). [a]Roman Numerals correspond to the experimental blocks from upslope to downslope. [b]Fractions in the following order: sand (2–0.02mm), silt (0.02–0.002mm), clay (<0.002 mm). [c] Intervals are for soil depth (cm). Values are mean±standard deviation (n is variable between 1 and 9). Sampling dates: May-2012 and May-2016).

Table 3. Summary of forest structure metrics in control and treated plots (C, T) for both sites (CAL: Calderona; HU: La Hunde). See text for abbreviations. Values between parentheses represent the average for each experimental block arranged from I to III (upslope to downslope). [§] represents values in 2016, [†] represents values in the year of treatment, [§†] represents values averaged along the total period.

Table 4. Rainfall and event-meteorology features of the Pg events studied in both study sites, Calderona (CAL) and La Hunde (HU) presented for convective (β≠0) and non-convective events (β=0), where β is the parameter indicative of the convective nature of an event. Pg: gross rainfall; P_D: event duration; P_I: mean intensity rate; P_{Imx}: maximum intensity rate; P_{Gap}, intra-event gaps; T: temperature; U: wind speed (maximum and average during the event); D: vapor pressure deficit. Only Pg>1 mm events were considered. Values reports are means; median and standard deviation in parenthesis. In HU from 1/Oct/12 to 30/Sep/16, P≤1mm: 220mm; In CAL from 1/Oct/13 to 30/Sep/16, P≤1mm: 94 mm).

Table 5. Summary of the statistical analyses (ANCOVA and Kruskal-Wallis) performed for the comparison between control (C) and treatment (T) plots in both sites (CAL and HU); *F* and *Chi* are the statistics used in the test; *, **, *** significance at p-levels ≤ 0.05, 0.01 and 0.001 respectively; df: degrees of freedom (factor, cases). $D_{BH}3/4$ refer to the diameter classes 3 and 4.

Table 6. Relative Importance from the BRT models fitted between the rainfall partitioning variables (throughfall, stemflow and interception) and the three sets of independent variables (rainfall, event-meteorology and forest structure, see Tables 2 and 3 for specific variables in each set). The importance, a relative term from 0 to 100, is computed as the scaled contribution of each specific variable to the improvement of the model. cv-correlation represents the cross-validation correlation coefficient of the fitted model.

FIGURE CAPTIONS

Figure 1. Localization of the experimental plots

Figure 2. Mean and median values in Calderona and La Hunde sites for the three variables selected to study the effect of forest management (thinning/clearing: T, control without management: C) on tree stemflow (Stf, l/tree) (left), stemflow coefficient (CStf, l/mm) (center) and, efficiency of stemflow (CStf_m^2, l/mm m^2) (right). Bars indicate the standard deviation. Different letters indicate significant differences between treatments. In La Hunde, differences in l/tree and l/mm are just for the bigger trees of diameter above 10.5 cm. Only P>1 mm considered.

Figure 3. Mean and median values in Calderona and La Hunde sites for throughfall, stemflow (on a ground basis) and interception either as depth (mm) or rates (as % of gross rainfall), as affected by forest management (thinning/clearing: T, control without management: C). Error bars indicate the standard deviation. Different letters indicate significant differences between treatments in a site.

Figure 4. Mean relative importance of the three sets of predictors (rainfall, event-meteorology and forest structure) for both depth (mm) and rate (% Pg) of Thr, Stf and It, after weighting with the cv correlation coefficient obtained in the BRT models in the study sites (HU, CAL and Overall).

Figure 5. Regressions of the event-based overall average of interception rate on forest structure: LAI and Cover (n=12; 6 blocks per site).

Figure 6. Partitioning of gross rainfall (Pg) in the throughfall (Thr), stemflow (Stf) and net rainfall (Pn) according to the water years, site and forest treatment.

Figure 7. Cumulative treatment impacts on the response variables (Stf, Thr and It) as shift of the daily ratio of treated/control (ln T/C) following the intervention (baseline before treatment is assumed to be zero).

Figure 8. Efficiency of thinning per unit of basal area (BA) or LAI removed on the reduction of the interception loss in the low biomass-forests studied here and in

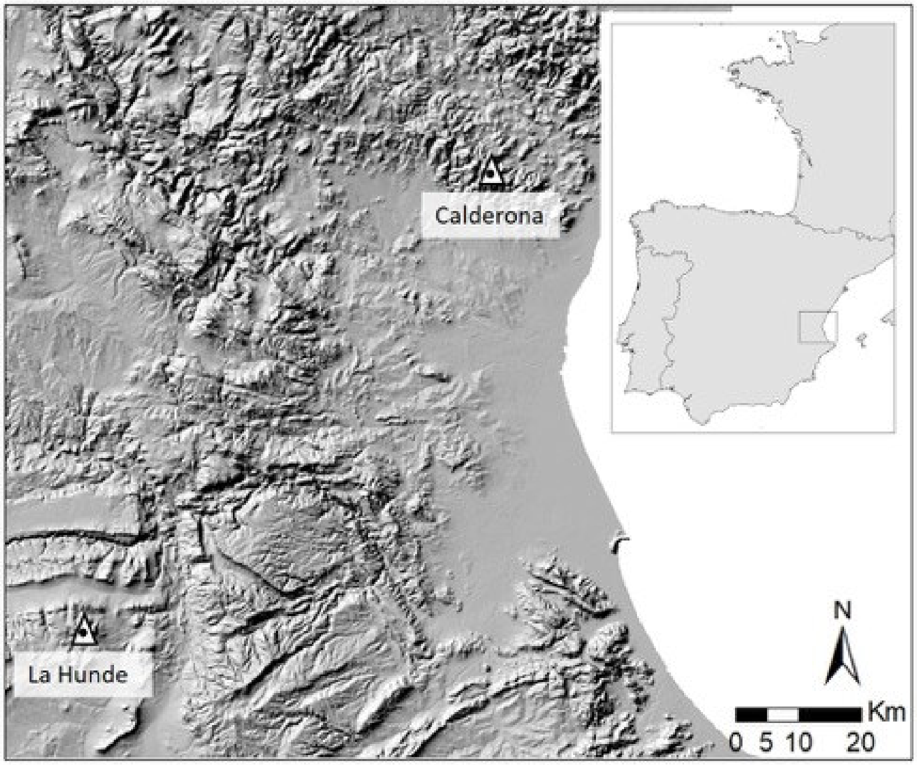
Calderona
La Hunde
N
Km
0 5 10 20

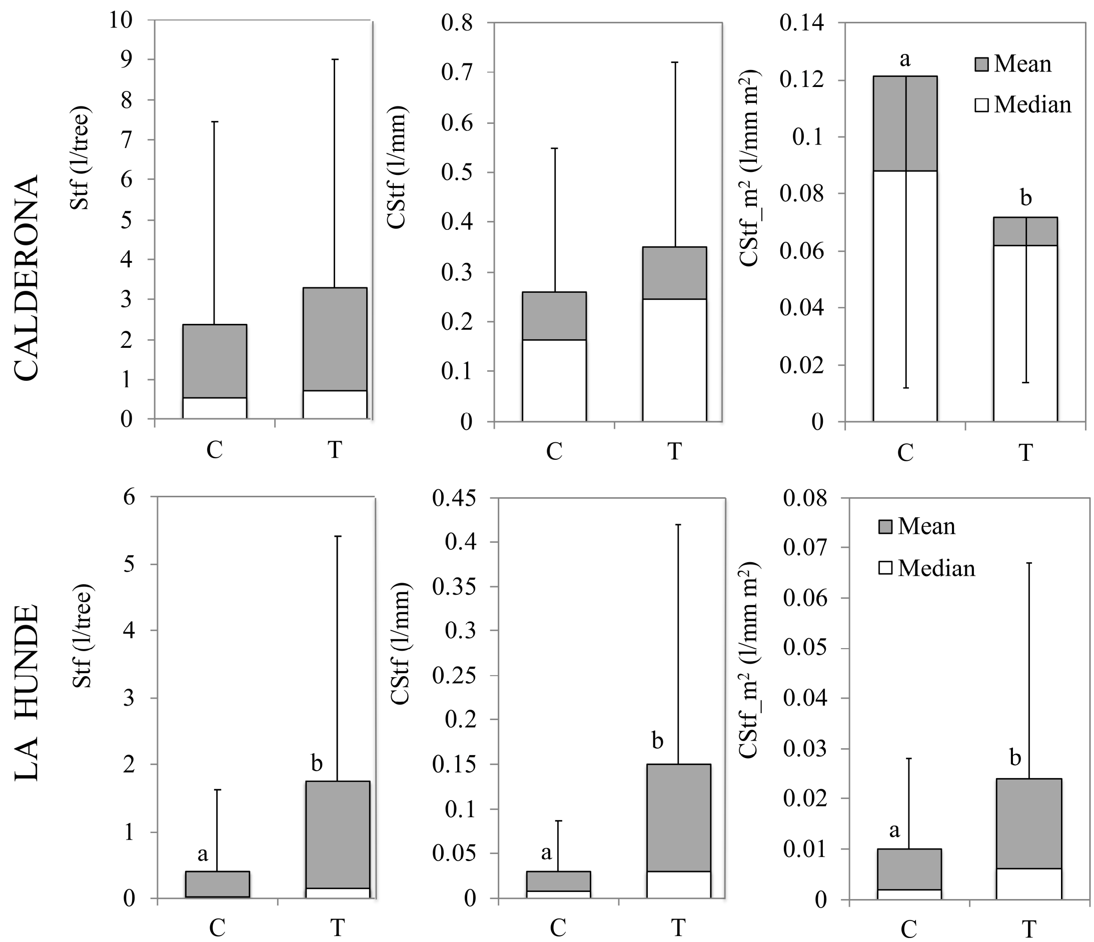
CALDERONA
LA HUNDE
Stf (l/tree)
CStf (l/mm)
CStf_m² (l/mm m²)
Mean
Median
C
T
a
b

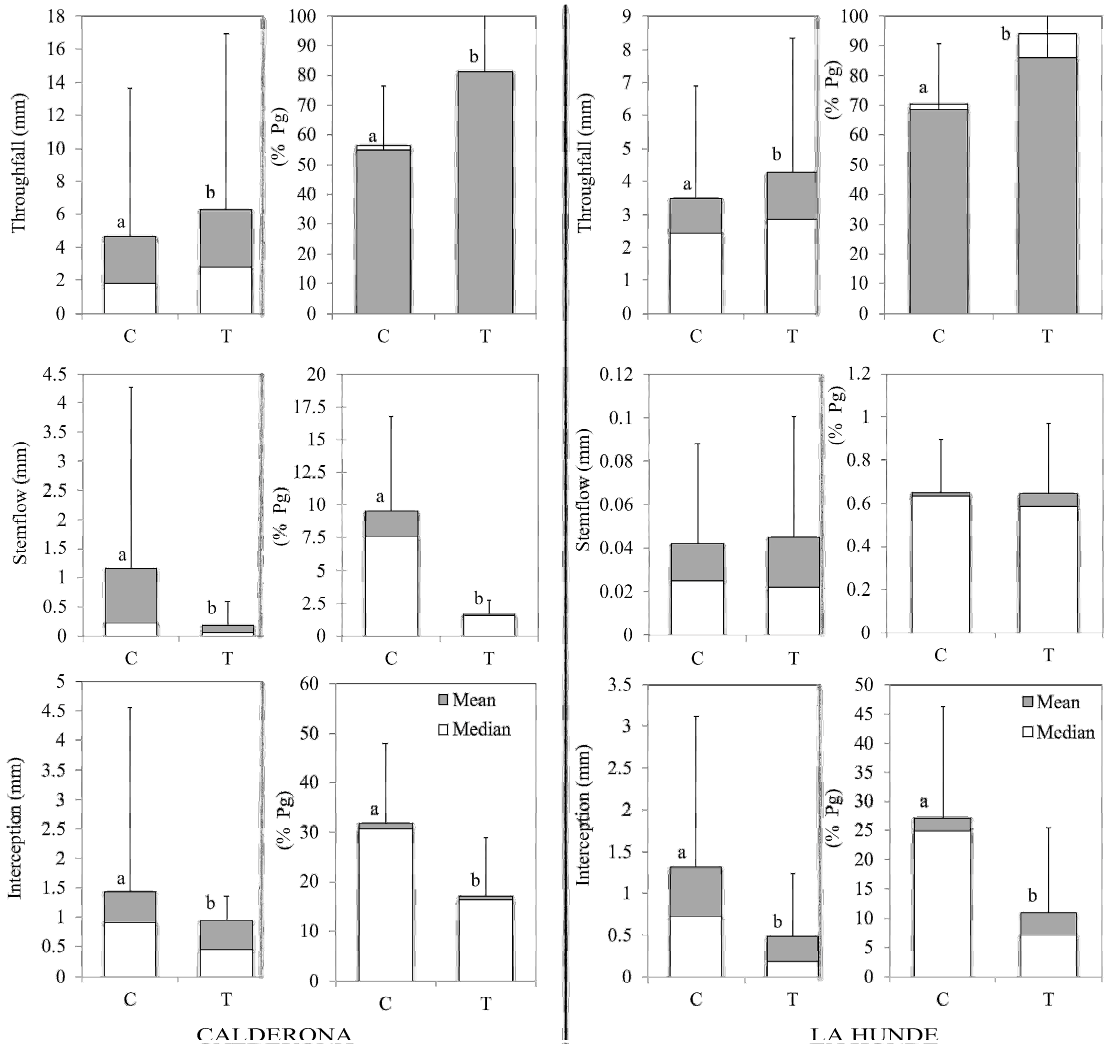

Throughfall (mm)
(% Pg)
Stemflow (mm)
Interception (mm)
Mean
Median
C
T
a
b
CALDERONA
LA HUNDE

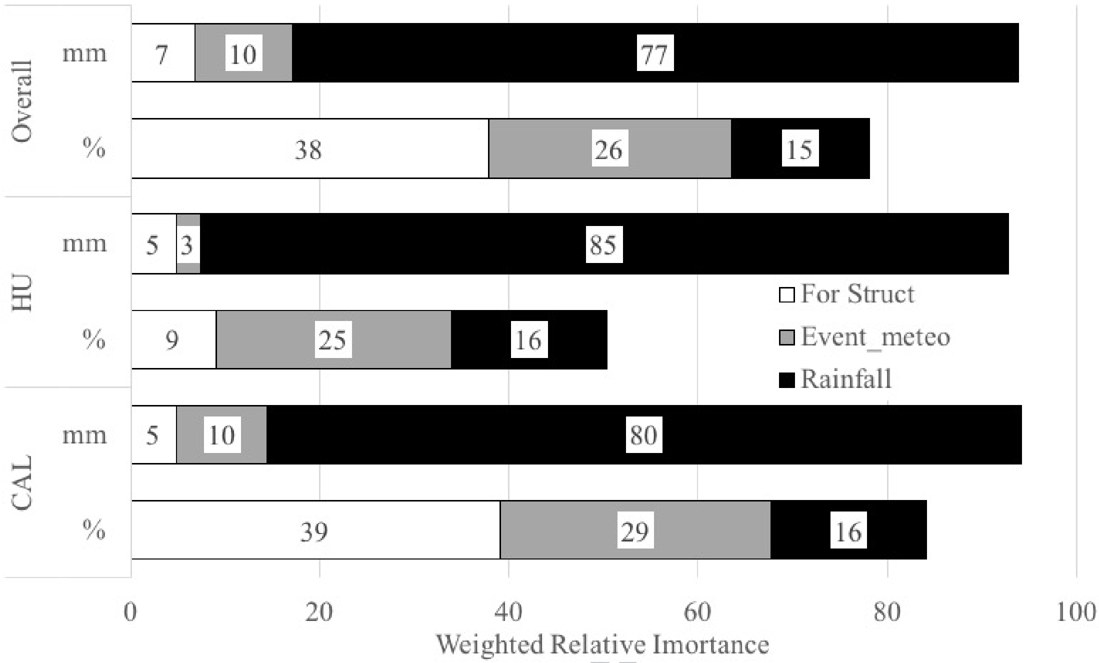
Overall
mm
7
10
77
%
38
26
15
HU
mm
5
3
85
%
9
25
16
CAL
mm
5
10
80
%
39
29
16
For Struct
Event_meteo
Rainfall
0
20
40
60
80
100
Weighted Relative Imortance

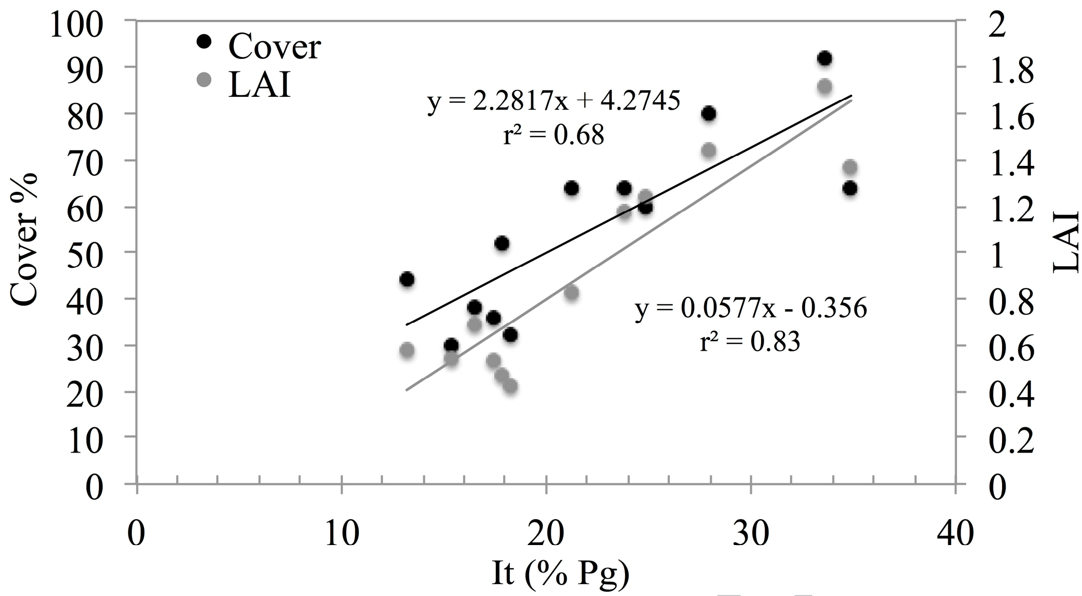

Cover
LAI
y = 2.2817x + 4.2745
r² = 0.68
y = 0.0577x - 0.356
r² = 0.83
Cover %
LAI
It (% Pg)
0
10
20
30
40
50
60
70
80
90
100
0.2
0.4
0.6
0.8
1
1.2
1.4
1.6
1.8
2

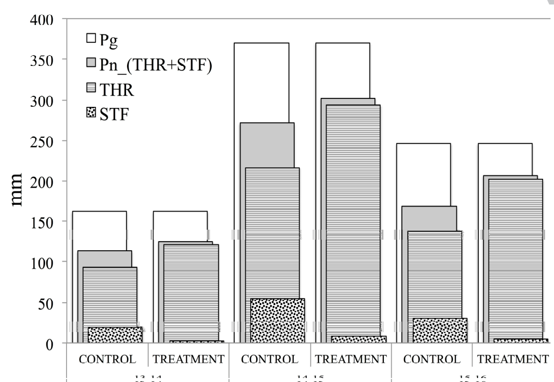

Pg
Pn_(THR+STF)
THR
STF
mm
CONTROL
TREATMENT
CONTROL
TREATMENT
CONTROL
TREATMENT
0
50
100
150
200
250
300
350
400

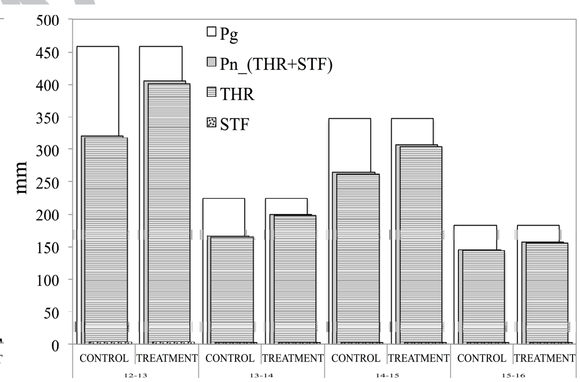

Pg
Pn_(THR+STF)
THR
STF
mm
CONTROL
TREATMENT
CONTROL
TREATMENT
CONTROL
TREATMENT
CONTROL
TREATMENT
12-13
13-14
14-15
15-16
0
50
100
150
200
250
300
350
400
450
500

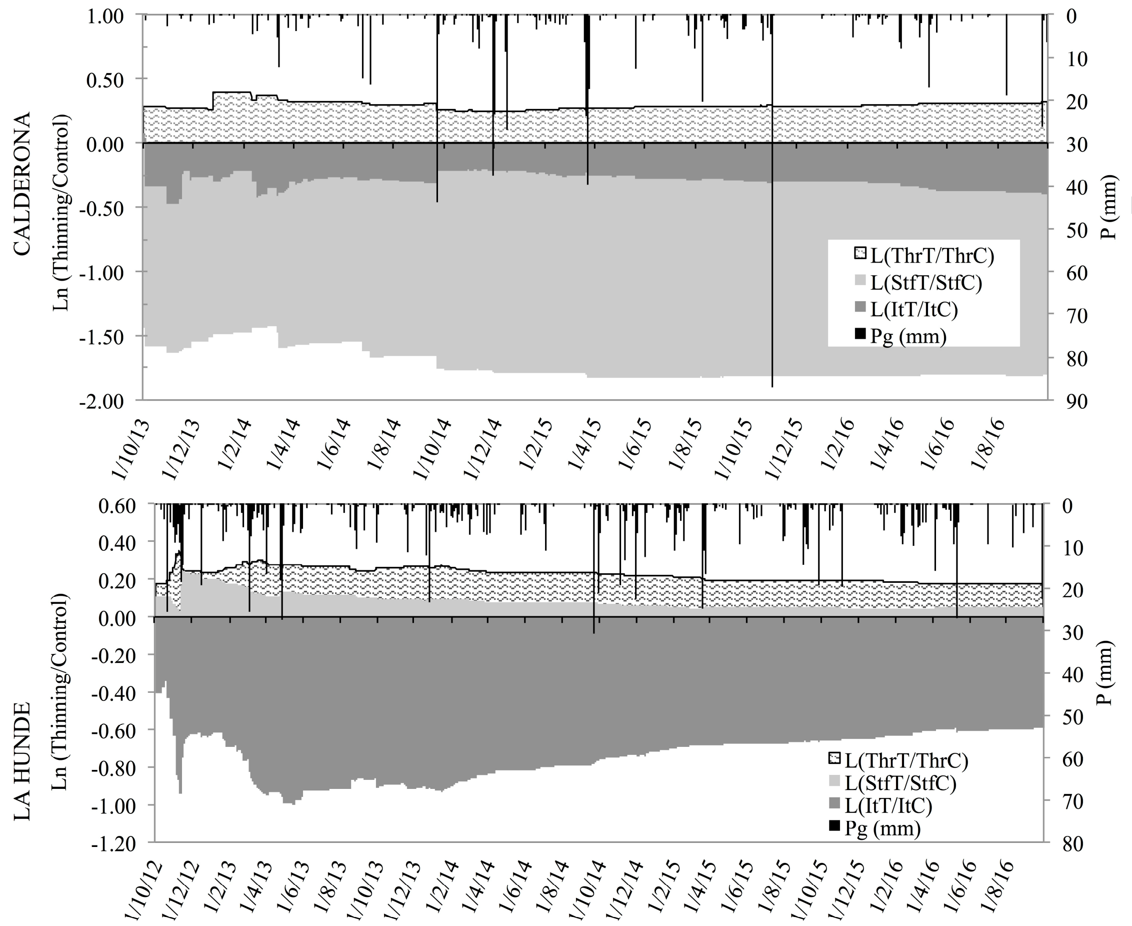
CALDERONA
Ln (Thinning/Control)
1.00
0.50
0.00
-0.50
-1.00
-1.50
-2.00
P (mm)
0
10
20
30
40
50
60
70
80
90
L(ThrT/ThrC)
L(StfT/StfC)
L(ItT/ItC)
Pg (mm)
1/10/13
1/12/13
1/2/14
1/4/14
1/6/14
1/8/14
1/10/14
1/12/14
1/2/15
1/4/15
1/6/15
1/8/15
1/10/15
1/12/15
1/2/16
1/4/16
1/6/16
1/8/16
LA HUNDE
Ln (Thinning/Control)
0.60
0.40
0.20
0.00
-0.20
-0.40
-0.60
-0.80
-1.00
-1.20
P (mm)
0
10
20
30
40
50
60
70
80
L(ThrT/ThrC)
L(StfT/StfC)
L(ItT/ItC)
Pg (mm)
1/10/12
1/12/12
1/2/13
1/4/13
1/6/13
1/8/13
1/10/13
1/12/13
1/2/14
1/4/14
1/6/14
1/8/14
1/10/14
1/12/14
1/2/15
1/4/15
1/6/15
1/8/15
1/10/15
1/12/15
1/2/16
1/4/16
1/6/16
1/8/16

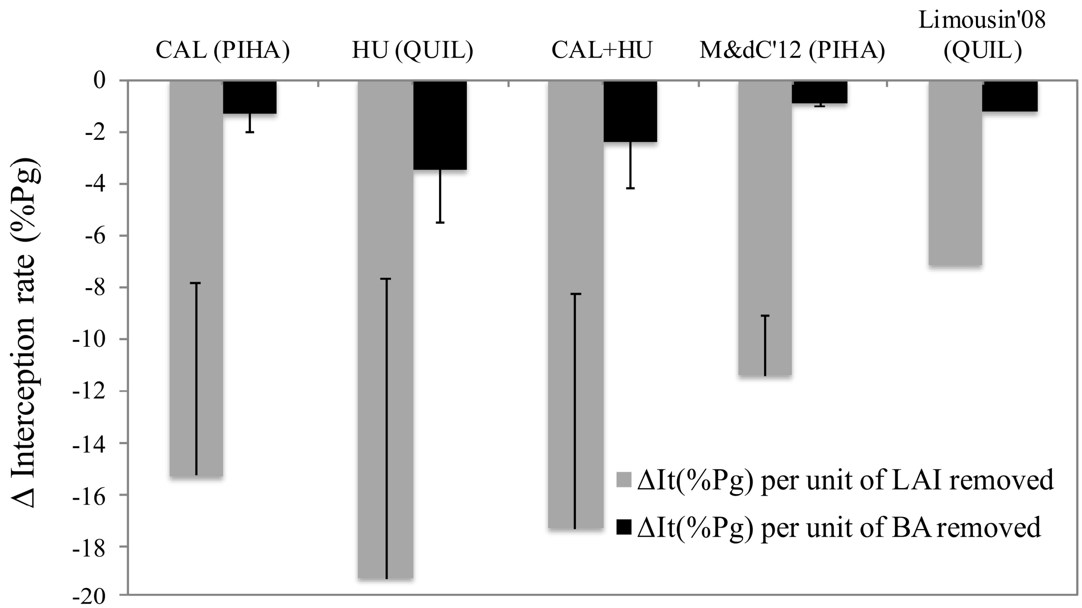
CAL (PIHA)
HU (QUIL)
CAL+HU
M&dC'12 (PIHA)
Limousin'08 (QUIL)
Δ Interception rate (%Pg)
0
-2
-4
-6
-8
-10
-12
-14
-16
-18
-20
ΔIt(%Pg) per unit of LAI removed
ΔIt(%Pg) per unit of BA removed

previous studies in both species (Molina and del Campo (2012), Aleppo pine; Limousin et al., (2008), Holm oak).

Table 1

Site, climate, country, P, T and forest-type	Length of the study period	Stand structure metrics	Driving variables explicitly addressed:	Effect of (adaptive) forest management	Reference
Upper Yass Representative Basin, oceanic climate, Australia (P: 679), dry sclerophyll eucalypt forest and pine plantation	7 years	D: 1525-1708 BA: 34-35	P-ev, P-met, FS	Thinning in a Pinus radiata plantation	Crockford & Richardson, 1990
Longmile, Rotorua, mild temperate climate, New Zealand (P: 1623, T:13), *Pinus radiata* plantation	2 years	D: 754 LAI: 4.9	P-ev, P-met, FS	Thinning in a Pinus radiata plantation	Whitehead, & Kelliher, 1991
Vallcebre catchment, Mediterranean mountain climate, Spain (P: 850, T: 9), monospecific stand of *Pinus sylvestris*	30 months	D: 2400 BA: 38	P-ev, P-met	Not considered	Llorens et al., 1997
Guadalperalon catchment, Mediterranean, Atlantic and continental climate, Spain (P: 516, T: 16), Open woodland (savannah-like) of *Quercus ilex*	3 years	D: 35-40	P-ev, P-met	Compare pruned and un-pruned trees.	Mateos & Schnabel, 2001
Puchabon State Forest, Mediterranean sub-humid climate, Southern France (P: 908, T: 13.5), dense coppice forest of *Quercus ilex* (clearcut in 1942)	12-24 months	D: 6885 LAI: 3.1	P-ev, P-met, FS	Combination of control, thinned (LAI: 1.6) and throughfall exclusion. Response to reduced P.	Limousin et al., 2008
Taxiarhis forest, temperate mesothermal climate, northern Greece (P: 980mm; T: 11.6 ºC), hardwood forest dominated by *Quercus frainetto*	24 months	D: 818-1825 BA: 9.3-36	FS	Hydrological impacts of thinning and clearcutting	Ganatsios et al., 2010
Vallcebre catchment, Mediterranean mountain climate, Spain (P: 850, T: 9), *Quercus pubescens* forest mixed with other deciduous species	30 months	D: 828 BA: 29 LAI: 3.35	P-ev, P-met, FS	Not considered	Mużyło et al., 2012
Yatir forest, Semiarid climate, Israel (P: 278, T:19.6), monospecific plantation of *Pinus halepensis*.	Dry/wet seasons	D: 300 BA: 6.7 LAI: 1.5	No Rainfall partitioning performed	Thinning discussed	Ungar et al., 2013
La Hunde public forest, semiarid continental Mediterranean climate, Spain (P: 465, T: 13.7), monospecific plantation of	27 months	D: 1289 BA: 36 LAI: 2.6	P-ev, FS	Thinning to different intensities	Molina & Del Campo, 2012; Del Campo et al., 2014

Pinus halepensis.					
Sardon catchment, semiarid Mediterranean climate, Spain (P:589, T:13.2), open woodland of *Quercus ilex* and *Q. pyrenaica*	2 years	D: 13 Cover: 7%	P-ev, P-met, FS	Not considered	Hassan et al., 2017
Sierra Calderona, semiarid Mediterranean climate (P:340, T:14), E Spain, dense sapling forest of *Pinus halepensis* regenerated after wildfire La Hunde public forest, semiarid continental Mediterranean climate, Spain (P: 465, T: 12.8), marginal oak coppice forest of *Quercus ilex*	3 / 4 years	D: 1155-11300 BA: 8.5-17 LAI: 1.1-1.5 Above-ground biomass: 23 MgC/ha	P-ev, P-met, FS	Thinning and shrub clearing treatments	This study

Table 2.

	Units	CAL		HU	
		0 (control)	1 (treated)	0 (control)	1 (treated)
Coordinates	Geographic	39º42'29-30" N 0º27'25-26" W	39º42'28-30" N 0º27'22-24" W	39º4'29-30" N, 1º14'25-26" W	39º4'48-49" N 1º14'46-48" W
Altitude	m a.s.l.	785-795		1080-1100	
Slope	%	26.8±6.5	28.9±10.3	30.8±6.0	33.1±7.9
Aspect	º (0º: east)	318.0±4.8	304.5±20.2	327.43+28.1	311.62+18.3
P (mm)	mm	342		466	
T (ºC)	ºC	14.0		12.8	
PET (mm)	mm	837		749	
Soil Depth[a]	cm	I:20;II:30;III:70		I:15;II:30;III:40	
Texture[b,c]	%	0-15: 45;29;26	0-15: 39;34;27	0-10: 44;33;23 10-30: 57;23;20 30-40: 48;32;19	
pH	(water)	8.3±0.2	8.3±0.1	7.9±0.2	8.0±0.1
Carbonates	(g g^{-1}dry soil)	0.319±0.154	0.371±0.114	0.215±0.096	0.260±0.042

Table 3.

Plot	D_B (cm)[§]	D_{BH} (cm)[§]	BA (m^2 ha^{-1})[†]	Density (tree ha^{-1})[†]	Cover (%)[§]	LAI (m^2 m^{-2})[†§]
LA HUNDE						
HU-C	11.87 (12.1;11.6;11.9)	8.62 (8.4;8.1;9.0)	8.5 (5.1;7.1;12.4)	1155 (875;1000;1460)	62.7 (60;64;64)	1.1 (1.24;0.83;1.18)
HU-T	18.09 (18.5;14.3;17.3)	14.18 (14.2;10.8;13.6)	4.98 (3.7;5.0;6.2)	310 (267;317;333)	39.3 (36;44;38)	0.6 (0.53;0.58;0.69)
CALDERONA						
CAL-C	4.33 (9.5;4.2;3.7)	2.74 (6.4;2.8;2.3)	17.5 (14.5;15.3;22.8)	11300 (3360;5188;25350)	78.7 (64;80;92)	1.5 (1.4;1.4;1.7)
CAL-T	13.18 (16.4;12.2;12.1)	8.51 (11.0;8.0;7.5)	4.54 (5.4;3.7;4.5)	703 (522;622;964)	38.7 (32;32;52)	0.5 (0.5;0.4;0.4)

Table 4.

Event convectivity	N	Total P (mm)	Event-rainfall characteristics						Event-meteorology			
			Pg (mm)	P_D (min)	P_I (mm/h)	P_{Imx} (mm/h, ΔT=10 min)	P_{Gap} (% events)	P_{Gap} (% time)	T (ºC)	D (Pa)	Umx (m/s)	Uav (m/s)
CALDERONA												
β=0	106	421	4.0 (2.6;3.9)	128 (91;118)	2.9 (2.1;3.2)	5.9 (4.8;4.7)	91	45	9.6	138	6.6	2.3
β≠0	10	262	26.2 (19.7;24.4)	171 (95;190)	12.4 (7.4;8.6)	40.4 (40.8;11.5)	100	20	13.3	227	10.9	3.7
LA HUNDE												
β=0	226	1136	5.0 (2.8;6.2)	240 (150;303)	1.7 (1.2;1.7)	4.1 (2.9;3.7)	67	40	8.1	127	3.5	0.7
β≠0	10	134	13.4 (12.4;8.0)	98 (83;73)	11.3 (9.8;7.0)	34.3 (31.5;11.1)	80	40	16.2	186	3.4	0.5

Table 5.

Site	Response variable	d.f.	F or *Chi*	Average: C - T, units
CALDERONA	Stemflow yield, Stf	1,900	1.31	2.4 - 3.3 l/tree
	Stemflow rate, CStf	1,900	1.48	0.26 - 0.35 l/mm
	Stf. funneling, $CStf_m{}^2$	1,900	5.97*	0.121 - 0.072 l/mm m^2
	Throughfall, mm	1,575	14.8***	4.66 - 6.26 mm
	Throughfall, %	1,575	182.1***	54.9 - 81.2 %
	Stemflow, mm	1,582	121.8***	1.15 - 0.18 mm
	Stemflow, %	1,582	348.9***	9.5 - 1.7 %
	Interception, mm	1,668	8.33**	1.42 - 0.94 mm
	Interception, %	1,691	163.0***	31.8 - 17.1%
LA HUNDE	Stemflow yield, Stf $D_{BH}3$	1,225	19.84***	0.29 -1.43 l/tree
	Stemflow yield, Stf $D_{BH}4$	1,209	8.01**	0.50 - 2.02 l/tree
	Stemflow rate, CStf $D_{BH}3$	1,225	46.98***	0.03 – 0.21 l/mm
	Stemflow rate, CStf $D_{BH}4$	1,209	5.90*	0.08 – 0.22 l/mm
	Stf. funneling, $CStf_m{}^2$	1,1098	46.07***	0.010 - 0.024 l/mm m^2
	Throughfall, mm	1,254	31.0***	3.49 - 4.27 mm
	Throughfall, %	1,254	50.0***	68.8 - 86.0%
	Stemflow, mm	1,464	1.22	0.042 - 0.045 mm
	Stemflow, %	1,464	0.44	0.65 - 0.64 %

	Interception, mm	1,337	69.4***	1.32 - 0.48 mm
	Interception, %	1,337	85.3***	27.1 - 11.0%

Table 6.

Site		cv correlation	Relative Importance (0-100)		
			Rainfall	Event-meteorology	For. Struct.
Overall	Thr, mm	0.992	91.7	7.2	1.2
	Stf, mm	0.922	75.8	16.5	7.7
	It, mm	0.901	76.8	9.7	13.5
	Thr, %	0.743	21.5	32.6	45.8
	Stf, %	0.947	10.5	24.6	64.9
	It, %	0.652	27.2	44.7	28.1
CAL	Thr, mm	0.993	90.9	8.1	1.0
	Stf, mm	0.913	77.0	16.2	6.8
	It, mm	0.921	85.4	6.6	8.0
	Thr, %	0.833	21.1	29.5	49.4
	Stf, %	0.936	13.0	28.9	58.1
	It, %	0.755	25.5	45.6	28.9
HU	Thr, mm	0.981	97.4	1.9	0.7
	Stf, mm	0.978	98.1	1.3	0.5
	It, mm	0.824	78.2	5.8	16.0
	Thr, %	0.485	30.6	46.4	23.0
	Stf, %	0.589	34.5	55.1	10.3
	It, %	0.434	31.3	46.3	22.5

Highlights

- Interception loss in low-biomass semiarid forests is higher than in mature closed forests
- Thinning reduced interception (It) more than 15% of Pg inter-annually
- Relative influence of forest structure and event meteorology in It was higher in a drier, warmer site.
- Gain in net P per unit of LAI removed (efficiency) was higher than for other forests/climates.